

DEFORMATION MECHANISMS IN ORDERED CuPt

A THESIS

Presented to
The Faculty of the Graduate Division
by

Henry Grady Paris


In Partial Fulfillment
of the Requirements for the Degree
Master of Science in Metallurgy


Georgia Institute of Technology

May 1973

DEFORMATION MECHANISMS IN ORDERED CuPt

Approved:


Chairman


Date Approved by Chairman 5/7/73

ACKNOWLEDGMENTS

In the long and fitful preparation of this work, the understanding, patience and support of several people merit acknowledgment. The transposition of this work from experimental notes to printed page occurred with guidance and helpful discussion with my thesis advisor, Dr. B. G. LeFevre. The helpful advise of my thesis advisory committee members, Dr. E. A. Starke, Jr., and Dr. Stephen Spooner is gratefully appreciated. Certain the aid and moral support of my fellow metallurgy graduate students must be gratefully acknowledged.

This research was made possible through the financial support of the Atomic Energy Commission Contract AT-(40-1)-3908.

TABLE OF CONTENTS

	Page
ACKNOWLEDGMENTS	iii
LIST OF TABLES	v
LIST OF FIGURES	vi
SUMMARY	vii
Chapter	
I. INTRODUCTION	1
A Review of the Structure and Mechanical Properties of Ordered Alloys The Structure of Ordered CuPt and Its Relation to Deformation Modes	
II. EXPERIMENTAL METHODS	12
Alloy Preparation and Ordering Rolling Transmission Electron Microscopy Techniques	
III. EXPERIMENTAL RESULTS	15
IV. DISCUSSION OF RESULTS AND CONCLUSIONS	28
V. RECOMMENDATIONS FOR FUTURE STUDY	31
APPENDIX	32
BIBLIOGRAPHY	38

LIST OF TABLES

Table	Page
1. The Four Types of Order Variants	5
2. The Effect of Partial Shears on the (111) Plane	8
3. Characteristics of Total and Partial Shears in the Four Order Variants of CuPt.	9
4. Orientation of Coherent Interfaces Between Adjacent Order Variants	42

LIST OF FIGURES

Figure	Page
1. Total Dislocation Motion on the (111) Plane in the Four Order Variants of Ordered CuPt Superlattice	6
2. Uniform Dislocation Tangles Interspersed Within an Order Variant.	17
3. $(\bar{1}11)$ Slip Bands in Ordered CuPt	18
4. Fine $(\bar{1}11)$ Deformation Bands in CuPt	19
5. Fine $(11\bar{1})$ Deformation Twins in Ordered CuPt	20
6. A (213) Selected Area Diffraction Pattern Displaying Twin Spots Resulting from $(11\bar{1})$ Deformation Twins	21
7. A Dark Field Image of $\{111\}$ Deformation Twins	23
8. Deformation Twins Lying on the $(11\bar{1})$ Nonlayered Planes in a Type 3 Order Variant Being Blocked by an Order Twin Boundary	24
9. A (011) Selected Area Diffraction Pattern of the Deformation Twins in Figure 8	25
10. A (011) Selected Area Diffraction Pattern of $(\bar{1}11)$ Deformation Twins Exhibiting Streaking Parallel to the Twin Axis	26
11. A Kikuchi Map of the Ordered CuPt Reciprocal Lattice	33
12. A Method of Identification of Order Variants in Ordered CuPt Using the (011) and (123) Selected Area Diffraction Patterns	40
13. A Method of Identification of Order Variants in Ordered CuPt Using the (112) and (123) Selected Area Diffraction Patterns	41

SUMMARY

Samples of ordered equiatomic CuPt have been reduced approximately 5% in thickness by cold rolling and the resultant substructure has been examined by transmission electron microscopy. Deformation was observed to occur by deformation twinning and planar slip. The deformation twinning occurred only on nonlayered $\{111\}$ planes in a manner which preserved the CuPt, $L1_1$, superlattice structure within the deformation twins. Intense planar slip was observed on both layered and nonlayered $\{111\}$ planes in coordination with the deformation twinning. Both slip and twinning were observed only to occur within single order variants, the order twin boundaries being a significant restraint on continuous deformation. A model is developed which explains the observed twinning and slip mechanisms in this alloy.

CHAPTER I

INTRODUCTION

A Review of the Structure and Mechanical Properties of Ordered Alloys

Many binary metallic solid solutions undergo an order-disorder transformation at some critical temperature, T_c , below the melting point. Below this critical temperature the atoms prefer specific lattice sites, producing a definite crystal structure described by long range order (1,2). Marked changes are frequently observed in the properties of these alloys upon a partial or total transformation to the ordered state by annealing below T_c . One of the significant changes occurs in the mechanical properties (3).

Changes in the mechanical properties of ordered alloys are related to the influence of the resulting crystal symmetry and microstructure on the deformation modes, slip and twinning. The two basic types of ordered crystal systems are the isostructural and neostructural systems (4,5). In the isostructural type, the crystal system remains the same as the disordered solid solution upon ordering. As a result of this type of ordering process only antiphase domains may form. In the neostructural alloys, adjacent domains may be rotated with respect to one another, creating a structure variously described as microtwins (6,7) transformation twins (6,8), mosaic structure (6,8), orientation variants (6,8) rotational domains (6), and order twins (9), depending on the author. In the isostructural alloys, the mechanical properties are

affected through changes in the dislocation character and the impediment to slip that is caused by antiphase boundaries (3). In neostructural alloys, two additional factors come into play: (i) the reduced symmetry makes the deformation twinning possible in addition to slip (3,10,11), (ii) the resultant twin boundaries make highly effective barriers to the deformation process by virtue of the rotated symmetry as well as the misfit resulting from transformation strains at the boundary (12,13). These factors will be discussed in relation to the CuPt structure in later sections.

The Structure of Ordered CuPt and Its Relation to Deformation Modes Crystallography and Microstructure

The crystal structure of ordered equiatomic CuPt has been determined as the rhombohedral $L1_1$, with alternating $\{111\}$ planes of Copper and Platinum (14,15). The transformation is accompanied by a lattice contraction perpendicular to the layered planes so the original rhombohedral angle of 90° becomes 91° (15). The resulting structure may be referred to an eight atom rhombohedral unit cell, or to a thirty-two atom pseudo-cubic unit cell having a lattice parameter of 7.58 \AA , twice the normal disordered face centered cubic unit cell. Since layering may occur on any of the four $\{111\}$ planes, four possible order variants may be present in the microstructure.

Fairly extensive studies of the ordering transformation in CuPt and its relationship to hardening have been conducted (9,11,16,17). It has been established by transmission electron microscopy that order twins occur on $\{100\}$ and $\{110\}$ habit planes in samples ordered near T_c

(9, 17). Antiphase boundaries occurring within the order twins were observed to coarsen with time along with the order twins. At low annealing temperatures the structure is complicated by the appearance of a coarse domained grain boundary component which resembles a recrystallized structure when observed optically.

Microhardness data on CuPt indicates that several mechanisms may operate during isothermal annealing (9). During the initial stages transformation strains associated with the high density of order twin boundaries appear to dominate. As the order twins coarsen with increased annealing time, the degree of long range order increases and the internal strains decrease.

Deformation Modes

When determining the deformation modes of an ordered structure the primary consideration is the periodicity of the superlattice. Shear vectors which produce slip or twinning are restricted in the early stages of deformation to those shears that maintain the original coordination of the A and B atoms. Consequently the allowable slip systems and twinning elements are more complicated than those for the disordered solid solutions.

It is well known that for a face centered cubic lattice the expected slip systems are the $\frac{1}{2} \langle 110 \rangle \{111\}$ and that the normal unit $\frac{1}{2} \langle 110 \rangle$ dislocation may dissociate into pairs of $\frac{1}{6} \langle 11\bar{2} \rangle$ partial dislocations with (either intrinsic or extrinsic) stacking fault ribbons between. Since extended dislocations have not been observed in our work on CuPt nor by Corke, et al. (18), we consider only unit and superdislocations in determining the slip systems for this structure.

Partial shears will be treated later in consideration of the deformation twinning modes.

The four order variants of CuPt may be defined as Type 1, 2, 3, and 4 according to the $\{111\}$ plane on which the layering occurs (9). These order variants are displayed in Table I. The allowable burgers vectors of the unit and superdislocations then can be determined by observing the atomic configuration for a given slip plane in the four different variants as depicted in Figure 1. Here it can be seen that while $\frac{1}{2} \langle 110 \rangle$ dislocations are sufficient for slip on the (111) plane in type 1 order variants, pairs of these dislocations (superdislocations in the $L1_1$ structure) may be required in the other three type order variants if the periodicity of the superlattice is to be maintained. Unit slip on either a layered or non-layered plane across an order twin boundary has only a probability of 1/3 for continuing without a change in burgers vector. Thus the impediment to slip presented by an order twin boundary is quite evident even without considering the lattice misfit in the interface. The experimental evidence is as predicted, that both unit and super-dislocations occur in this structure and that the dislocations do, in fact, change character at an order twin boundary (11, 18).

Deformation twinning in face centered cubic lattices can occur by repeated $1/6 \langle \bar{1}12 \rangle \{111\}$ partial shears on successive planes, or by extrinsic shears on every other plane. Only intrinsic shears will be considered since they are energetically much more favorable (24,25). For successive intrinsic shears on the $\{111\}$ planes there are two possibilities: (i) both the fundamental lattice and the superlattice

Table 1. The Four Types of Order Variants

ORDER TWIN TYPE	{111} LAYERING PLANE
Type 1	(111)
Type 2	(11 $\bar{1}$)
Type 3	($\bar{1}$ 11)
Type 4	(1 $\bar{1}$ 1)

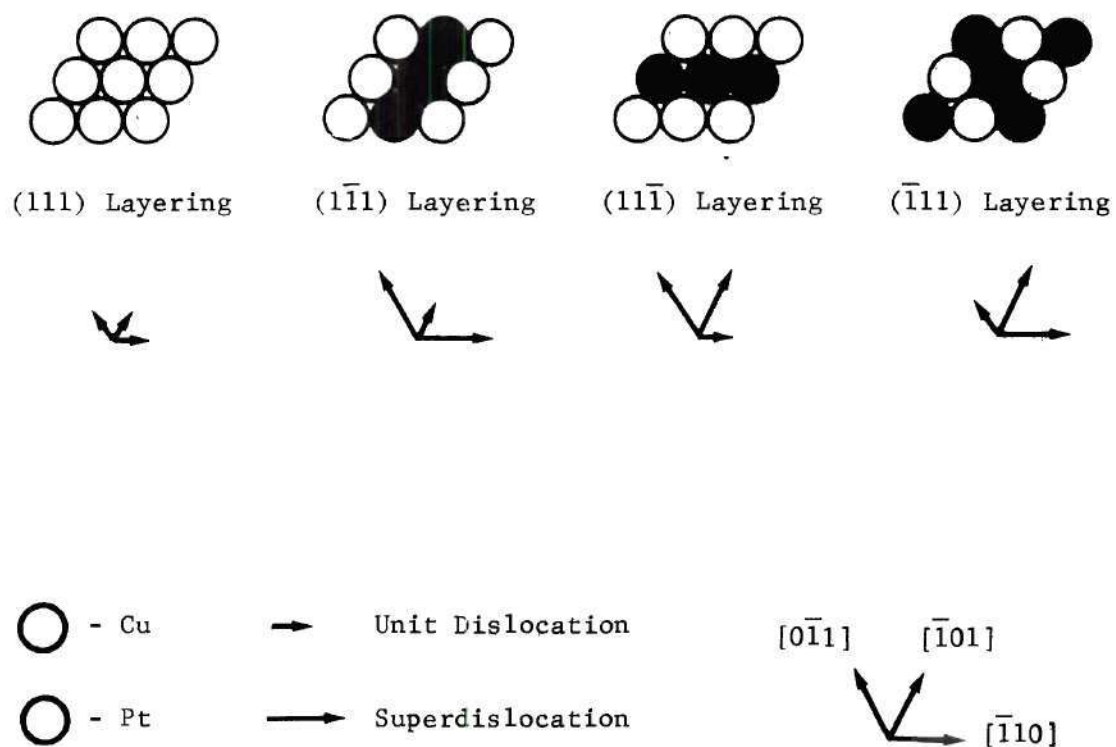


Figure 1. Total Dislocation Motion On The (111) Plane In The Four Order Variants Of Ordered CuPt.

will be twinned as by a 180° rotation about the proper $[111]$ pole or (ii) each shear produces an antiphase boundary of the type that transforms the CuPt superlattice ($L1_1$) into the CuAuI superlattice ($L1_0$). These possibilities are depicted in Table 2, where the effect of intrinsic shears on the (111) plane is considered in each of the four types of order variants. In type 1 variants all three intrinsic shears occur on a layered plane and product twinned superlattice structure, whereas in each of the three remaining variants only one of the three possible intrinsic shears on the (111) plane will produce a twinning $L1_1$ superlattice structure. The other two shears produce an $L1_0$ superlattice structure. This result is the inverse of that shown by Pashley and coworkers in considering twinning in the $L1_0$, CuAuI, superlattice structure(10). One would not expect twinning to occur on the layered plane where unit slip is unrestricted since for small amounts of work hardening slip is expected to be a preferred mode of deformation over twinning. For the nonlayered planes, twinning is possible provided the proper $\langle 112 \rangle$ shear operates. Those shears which produce the $L1_0$ structure are restricted because they are energetically unfavorable.

The above discussion points out the nature of the geometric restrictions on slip and twinning modes in the CuPt superlattice structure by a consideration of specific planes and directions of shear. Crystallographic multiplicity also must be taken into account in any real deformation process. This is done in Table 3 where all possible planes and directions of shear are considered in each of the four variants. The impeding effect of an order twin boundary can readily

Table 2. The Effect of Partial Shears on the (111) Plane

Order Variant	Partial Shears on the (111) Plane		
	a/6 $[11\bar{2}]$	a/6 $[1\bar{2}1]$	a/6 $[\bar{2}11]$
(111)	Twinned CuPt (111) layering	Twinned CuPt (111) layering	Twinned CuPt (111) layering
($11\bar{1}$)	Twinned CuPt (111) layering	Twinned CuAuI (001) layering	Twinned CuAuI (001) layering
($\bar{1}11$)	Twinned CuAuI (100) layering	Twinned CuAuI (100) layering	Twinned CuPt (111) layering
($1\bar{1}\bar{1}$)	Twinned CuAuI (010) layering	Twinned CuPt (111) layering	Twinned CuAuI (010) layering

Table 3. Characteristics of Total and Partial Shears in the Four Order Variants of CuPt.

Shear Plane	Shear Vector	Order Variant			
		Type 1 (111)	Type 2 (111)	Type 3 (111)	Type 4 (111)
(111)	$[0\bar{1}1]$	Unit	S.D.	Unit	S.D.
	$[\bar{1}01]$	Unit	S.D.	S.D.	Unit
	$[\bar{1}\bar{1}0]$	Unit	Unit	S.D.	S.D.
	$[11\bar{2}]$	CuPt	CuPt	CuAuI	CuAuI
	$[1\bar{2}1]$	CuPt	CuAuI	CuAuI	CuPt
	$[\bar{2}11]$	CuPt	CuAuI	CuPt	CuAuI
$(11\bar{1})$	$[011]$	S.D.	Unit	S.D.	Unit
	$[101]$	S.D.	Unit	Unit	S.D.
	$[\bar{1}\bar{1}0]$	Unit	Unit	S.D.	S.D.
	$[\bar{1}\bar{1}\bar{2}]$	CuPt	CuPt	CuAuI	CuAuI
	$[\bar{1}\bar{2}1]$	CuAuI	CuPt	CuPt	CuAuI
	$[2\bar{1}\bar{1}]$	CuAuI	CuPt	CuAuI	CuPt
$(\bar{1}11)$	$[0\bar{1}1]$	Unit	Unit	Unit	S.D.
	$[101]$	S.D.	S.D.	Unit	S.D.
	$[\bar{1}\bar{1}0]$	S.D.	S.D.	Unit	Unit
	$[1\bar{1}\bar{2}]$	CuAuI	CuAuI	CuPt	CuPt
	$[12\bar{1}]$	CuAuI	CuPt	CuPt	CuAuI
	$[\bar{2}11]$	CuPt	CuAuI	CuPt	CuAuI
$(\bar{1}\bar{1}1)$	$[\bar{1}\bar{1}0]$	S.D.	Unit	S.D.	Unit
	$[\bar{1}\bar{1}01]$	Unit	S.D.	S.D.	Unit
	$[011]$	S.D.	S.D.	Unit	Unit
	$[\bar{1}\bar{1}\bar{2}]$	CuAuI	CuAuI	CuPt	CuPt
	$[\bar{1}\bar{2}1]$	CuPt	CuAuI	CuAuI	CuPt
	$[21\bar{1}]$	CuAuI	CuPt	CuAuI	CuPt

be seen by noting the change in the character of a particular shear mode upon crossing from one variant into another.

The information in Table 3 can be summarized as follows:

i) Superdislocations are not required on layered $\{111\}$ planes and only unit dislocations are expected. Both unit and superdislocations may propagate on nonlayered $\{111\}$ planes.

ii) A unit dislocation propagating on a layered or nonlayered $\{111\}$ plane has a probability of .67 for changing to a superdislocation when crossing an order twin boundary.

iii) A superdislocation has a probability of .33 for maintaining its character upon crossing an order twin boundary and a probability of 0.67 for changing into unit dislocations.

iv) Intrinsic $1/6 \langle 11\bar{2} \rangle$ shears may operate on either layered or nonlayered $\{111\}$ planes to produce a twinned CuPt superlattice ($L1_1$) structure. On the nonlayered $\{111\}$ planes, only one of the three intrinsic shears retains the $L1_1$ superlattice structure whereas all three shears retain the $L1_1$ superlattice structure on the layered $\{111\}$ planes.

v) A twinning shear on a nonlayered $\{111\}$ plane consequently cannot propagate across an order twin boundary without producing the $L1_0$ superlattice structure unless the shear plane in the adjacent variant is a layered $\{111\}$ plane. This has a probability of 0.33 for occurring; however, on the layered plane, only unit slip is expected. As a result, deformation twins are not expected to occur on the layered plane, or to propagate across an order twin boundary.

In the preceding discussion the deformation modes of ordered CuPt were treated in terms of periodicity requirements only. In an actual

deformation process the additional factors of critical shear stresses and lattice misfit at order twin boundaries are important. These latter factors will be considered in the discussion of results.

CHAPTER II

EXPERIMENTAL PROCEDURE

Alloy Preparation and Ordering

The starting material for this study was a well homogenized ingot prepared by Richard Mitchell in a previous study of ordering kinetics of CuPt (9). The ingot was prepared from Cu and Pt of 99.999% and 99.99% purities, respectively, by arc melting. The ingot's dimensions were 12 x 6 x 6 mm. It was cleaned and subsequently encapsulated in Vycor tubing at reduced pressure ($\sim 10^{-6}$ torr) for an ordering treatment. The encapsulated specimen was placed in a horizontal Hevi Duty Lindburg Furnace and the temperature was raised to 850°C and held for fifteen minutes to disorder the sample. Subsequently the temperature was lowered to 700°C and held for one week and then the furnace was cooled to room temperature.

Rolling

After the ordering treatment the sample was removed from the capsule and wet ground on 600 grit silicon carbide paper to produce parallel surfaces for rolling. The sample was then lightly cold rolled in two passes to a total reduction in thickness of $\sim 5\%$.

Transmission Electron Microscopy Techniques

The deformed sample was oriented such that slices were abrasive and spark cut parallel to the rolling and normal directions and perpen-

dicular to the transverse direction. The slices were carefully wet ground to either 0.051 mm or 0.127 mm thickness, and discs 2.3 mm in diameter were spark trepanned from them for preparation of thin foils.

Thin foils were prepared by both electropolishing and ion milling techniques. The electropolished foils were prepared by a previously described method (9) which is a modification of the methods of Dewey and Lewis (19) and DuBose and Steigler (20). Black anodic deposits resulting from this electropolishing procedure were present on most of the prepared electropolished foils. This deposit was extremely difficult, if not impossible, to remove while simultaneously preserving the quality of the thin foils. To solve this problem the electropolish technique was abandoned and foils were prepared by an ion milling technique [courtesy of the University of Florida, Materials Research Laboratory] from the 0.051 mm thick discs. This method produced foils which possessed slightly larger transparent areas, but most importantly, foils were free of any contaminating anodic deposits.

The foils were examined at 125 Kv accelerating potential in a Siemens Elmiskop IA equipped with a precision dark field attachment and a Swann tilting stage having a $\pm 20^\circ$ tilt about two orthogonal axes. (Due to certain limitations of the foils and the tilting stage, full tilt could not be achieved in most cases.)

The observed structure was analyzed by the use of standard methods of bright field-dark field imaging, trace analysis, and analysis of selected area diffraction patterns. The use of these techniques as well as the theory of image contrast and diffraction effects of electrons in thin metallic foils is described extensively by several authors

(21,22,23). The identification of order variants from selected area diffraction patterns is an essential part of the analysis required to differentiate among the various deformation mechanisms proposed in the previous section. The techniques for this are rather detailed and therefore included in the appendix.

CHAPTER III

EXPERIMENTAL RESULTS

Examination of the deformed CuPt alloy in the transmission electron microscope revealed a variety of microstructural features associated with deformation processes. The more distinct features were:

i) Regions of uniform dislocation tangles comprised of primarily unit dislocations.

ii) Slip bands on $\{111\}$ planes comprised of a high density of dislocations many of which were in apparent screw orientation.

iii) Deformation twins on $\{111\}$ planes ranging in thickness from a few Angstroms to approximately 0.1μ .

iv) Unit and paired dislocations which appeared to be associated with slip bands and deformation twins. The density of unit dislocations far exceeded the density of paired dislocations.

Examples illustrating these features will be presented in the following paragraphs. For many of the fine "deformation" bands found on $\{111\}$ planes a clear differentiation between slip bands and twins was not possible, either on the basis of image contrast or selected area diffraction, however, both these features were clearly identified in certain areas of the foils. Although unit and paired dislocations were found in areas of the foils, it was not possible to determine burgers vectors in situations where the slip plane trace was distinct. Part of the difficulty arose from limitations of the tilting stage and the

quality of the foils attainable with CuPt. However, the characteristics of the deformation process contributed to the difficulty of interpretation. It was found, for example, that in virtually all cases where the slip plane was distinct, the dislocation density was too high for individual burgers vectors to be resolved even at this low amount of deformation.

An area of uniform dislocation tangles is shown in Figure 2. As seen in this micrograph these areas often appeared inside single order twin boundaries.

Examples of slip bands lying on $\{111\}$ planes are shown in Figure 3. Numerous paired dislocations can be seen. It is apparent that more than one slip system is operative so that it is difficult to associate specific dislocations to specific planes. The paired dislocations are presumably superdislocations comprised of $1/2 \langle 110 \rangle$ unit dislocations. Many of the superdislocation appear to have cross slipped onto intersecting slip planes. Note, for example, the dislocations connecting the thin bands in Figure 3. A high density of screw dislocations would be necessary for such a cross slip process.

Similar regions are presented in Figures 4 and 5. As mentioned earlier, it was not always possible to determine if deformation twins were present. In figure 4, no twin spots attributable to deformation twinning were obtained in the selected area diffraction pattern of the features, whereas in Figure 5, the nearly vertical striations such as along AA' did produce definite twin spots in selected area diffraction patterns of the features. In Figure 6, the diffraction pattern from these features in Figure 5 is presented with spots properly indexed



1.0 μ

Figure 2. Uniform Dislocation Tangles Interspersed within an Order Variant.

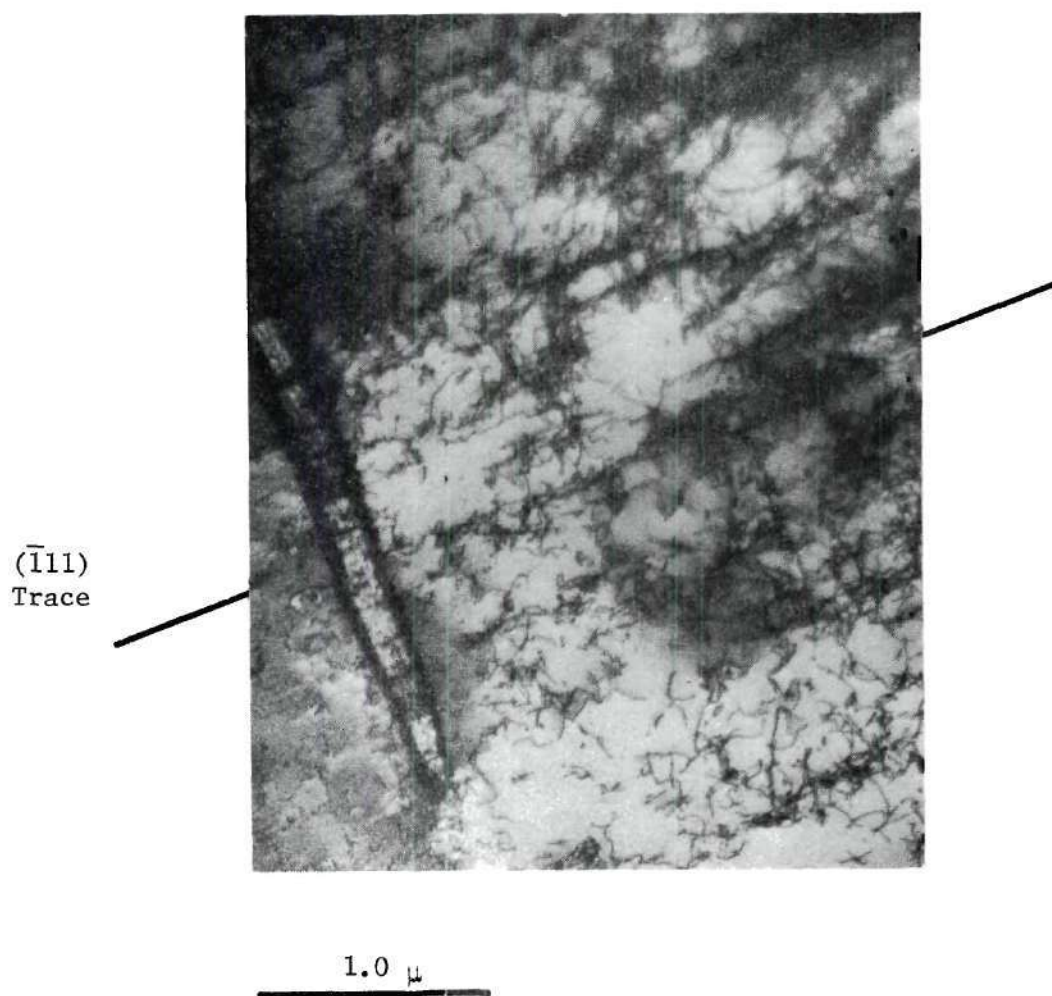


Figure 3. ($\bar{1}11$) Slip Bands in Ordered CuPt. The Order Variant is Type 4, (111) Layering. Consequently, the Slip Bands are on a Nonlayered Plane.

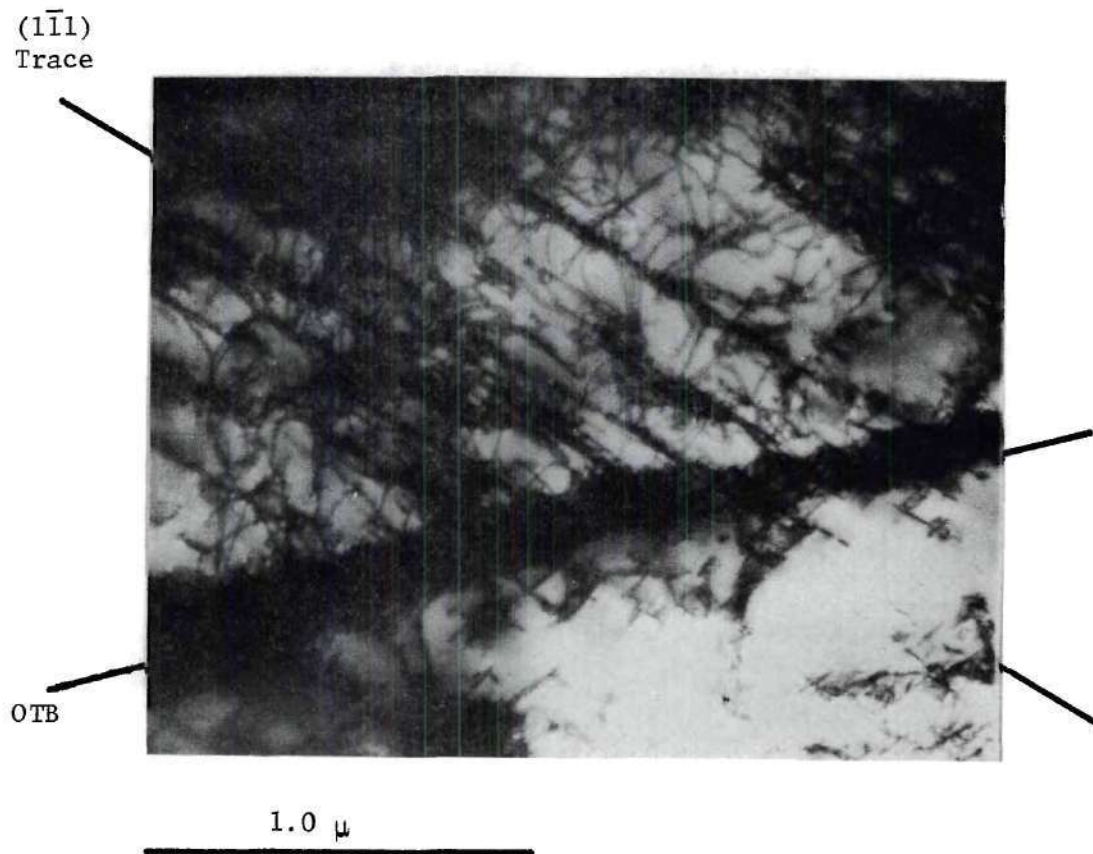


Figure 4. Fine Deformation Bands in Ordered CuPt. The Paired Dislocations Lie on Either (111) or (111) Planes. The Slip Bands Lie on a Nonlayered Plane.



Figure 5. Fine Deformation Twins on $(11\bar{1})$ Planes. Although the Order Variant Identity is Unknown, the $(11\bar{1})$ is a Nonlayered Plane as Shown in Figure 6, a Diffraction Pattern of these Features.

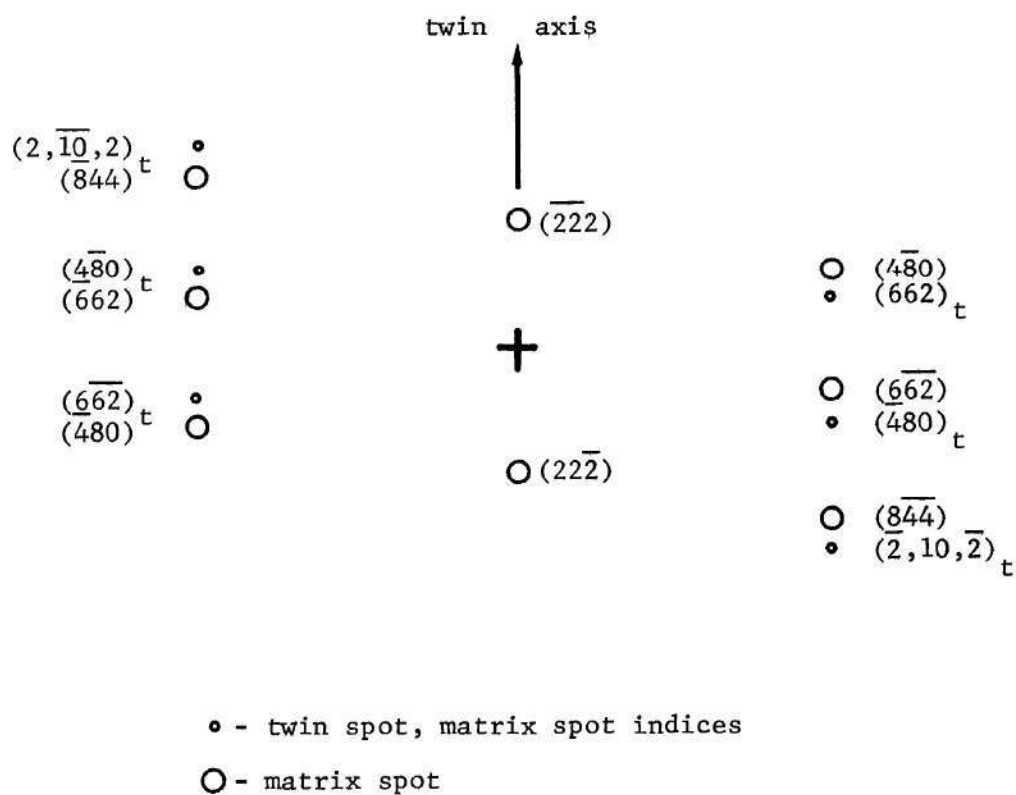


Figure 6. A Graphic Presentation of a (213) Selected Area Diffraction Pattern From the Twinned Region of Figure 5. Note the Crystallographic Indices Refer to the Enlarged Pseudocubic Unit Cell. The Twin Axis Is Perpendicular to a Nonlayered Plane.

and the twin axis identified. This figure illustrates a feature that was consistently observed in these foils. The $\{111\}$ deformation twins lie on nonlayered planes and the twin-axis is perpendicular to these planes. This observation is in agreement with the predictions treated earlier in Chapter I on the deformation modes. Further examples of $\{111\}$ deformation twinning are shown in Figure 7.

Impediment to deformation shears by order twin boundaries was generally observed. This is illustrated in Figure 8, where the deformation twins in variant "A" (type 3) stop at the order twin boundary separating variant "B" (type 4) from variant "A". In variant "B", the nearly vertical bands are slip bands lying on a $(\bar{1}11)$ nonlayered plane.

In Figure 9, the selected area diffraction pattern from variant "A" shows that the twinning shear plane is a nonlayered plane, and that the superlattice in the deformation twins is rotated intact about the twin axis along with the fundamental lattice. This can only occur if the proper partial shear operates on the nonlayered plane. A similar diffraction pattern, Figure 10, taken from an area of very fine twins contained streaks parallel to the twin axis. This is further confirmation that the striations in Figure 10 are indeed fine deformation twins.

In the observed foils, the predominant mode of deformation took the form of planar slip bands and fine deformation twins always occurring on nonlayered planes and restricted by order twin boundaries to single variants. The identifiable slip traces were found on both layered and nonlayered $\{111\}$ planes with paired dislocations present. Although the paired dislocations were presumed to lie on nonlayered planes where superdislocations might be required, this fact was not unambiguously estab-

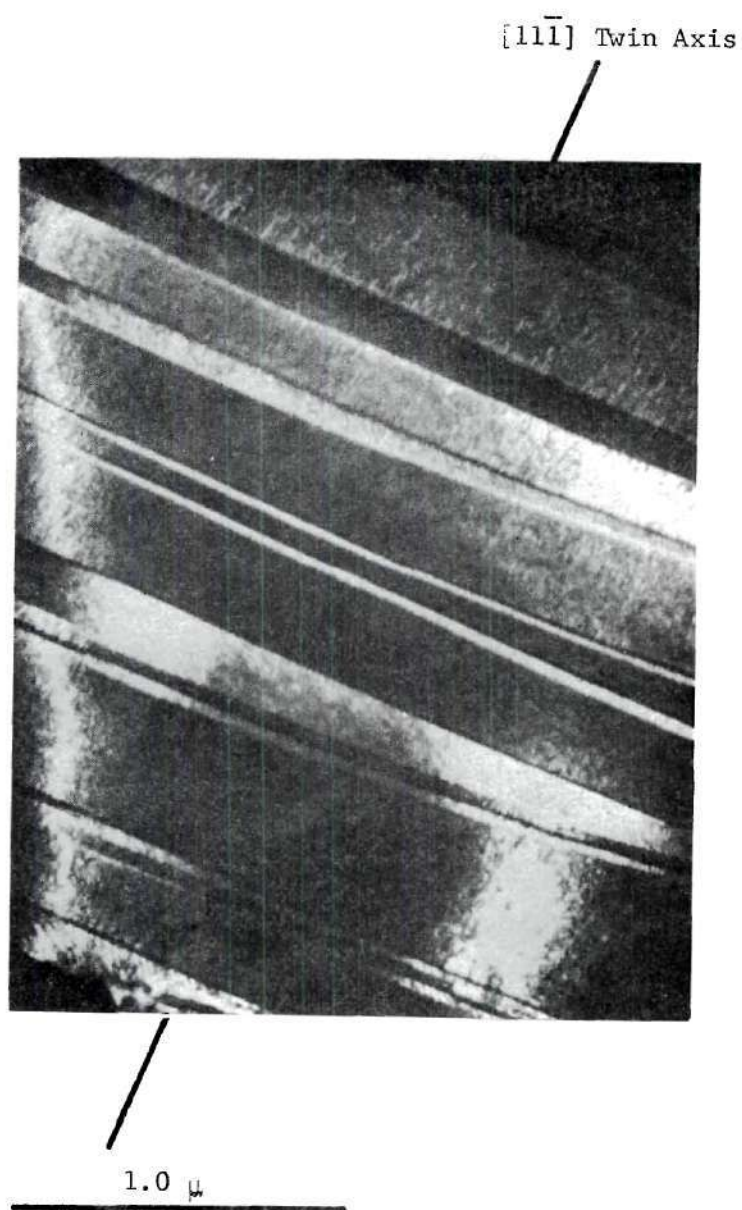


Figure 7. A Dark Field Image Showing $\{111\}$ Deformation Twinning in Ordered CuPt. The Order Variant is Type 4 and the Twins Lie on the (111) Nonlayered Plane.

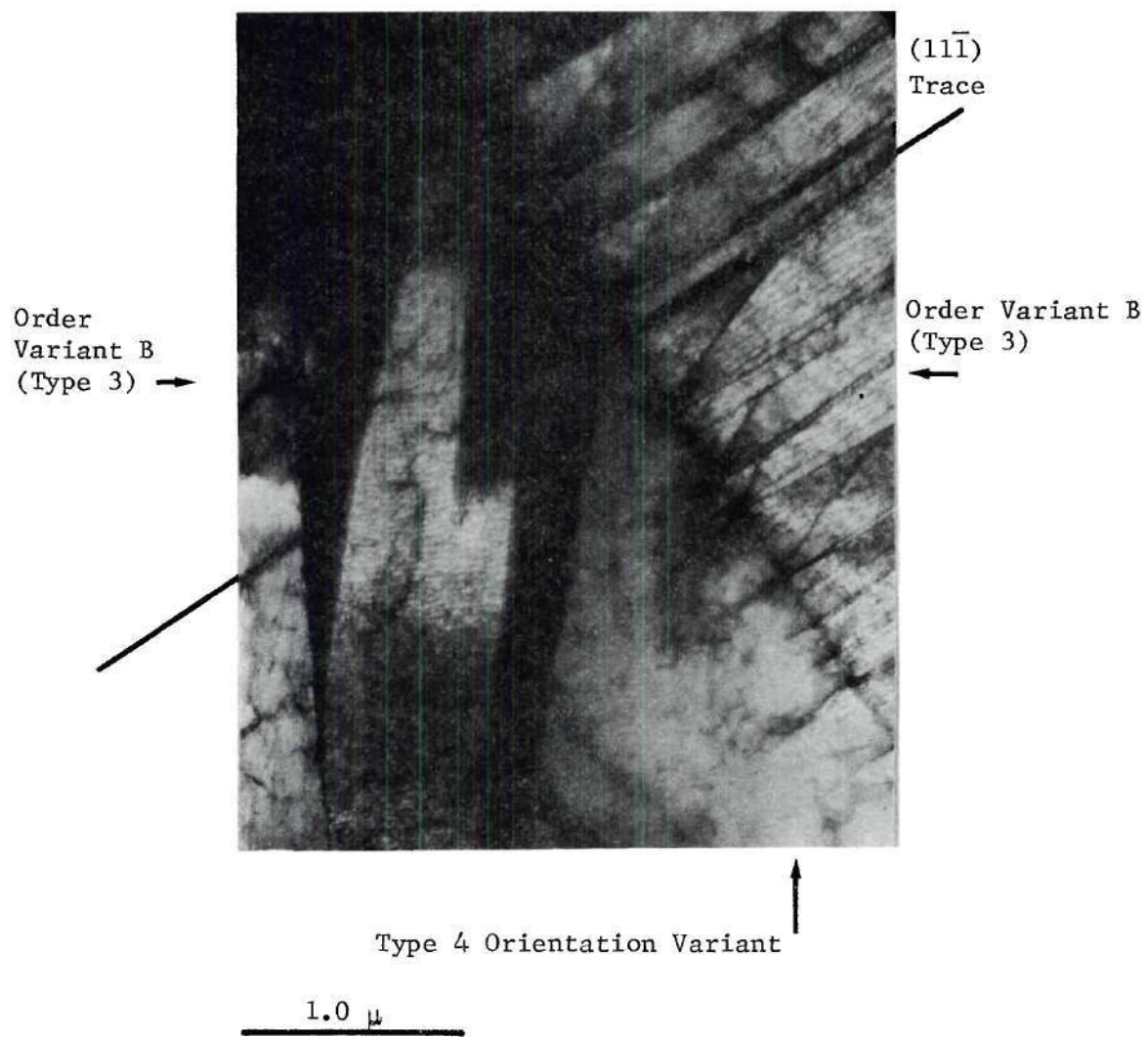


Figure 8. Deformation Twins on $(11\bar{1})$ Nonlayered Planes in Variant A being Blocked at an Order Twin Boundary.

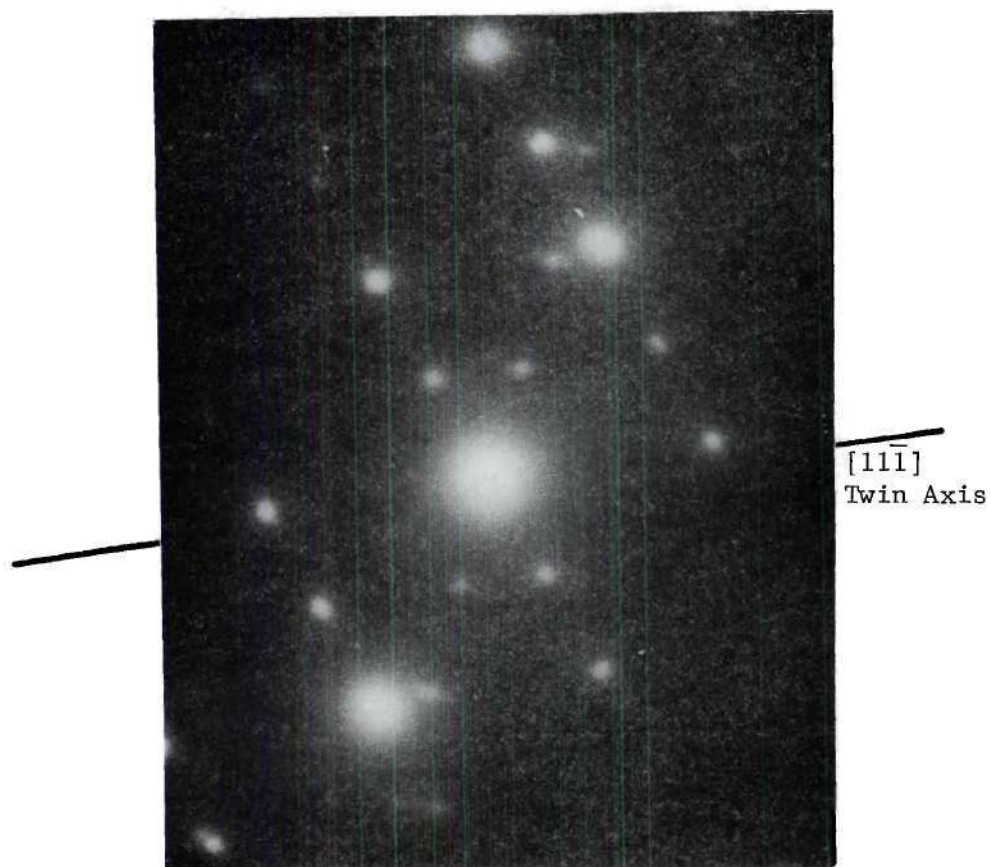


Figure 9. Selected Area Diffraction Pattern of the Deformation Twins in Figure 8. The Twin Axis is Perpendicular to the Nonlayered Twin Plane. Both Fundamental and Superlattice Spots are Rotated 180° about the Twin Axis to Create the Twin Spots.

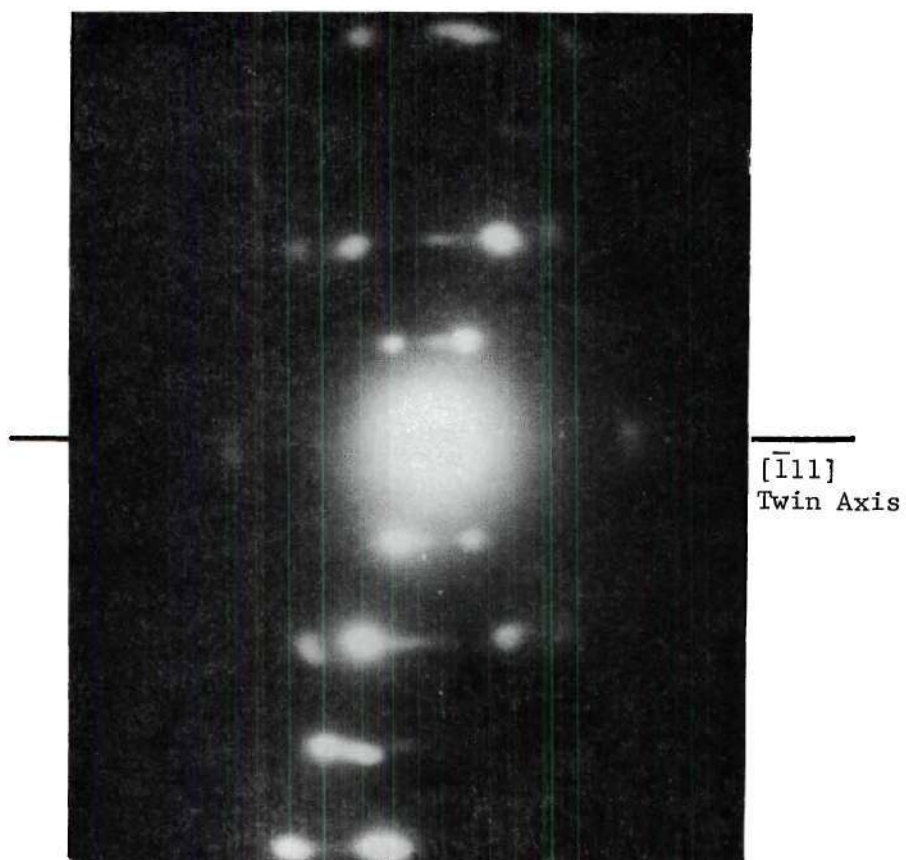


Figure 10. A (011) Selected Area Diffraction Pattern of $(\bar{1}11)$ Deformation Twins Exhibiting Streaking Parallel to the Twin Axis.

lished. At points along the order twin boundaries where $\{111\}$ deformation twins were impeded, deformation progressed into the adjacent variant by slip on either a parallel or inclined $\{111\}$ plane. It appeared that the bulk of the deformation proceeded by slip on inclined planes. That is, as Figure 8 shows, the shear vector tended to change directions on encountering an order twin boundary.

CHAPTER IV

DISCUSSION OF RESULTS AND CONCLUSIONS

The preceding observations on the plastic deformation behavior of CuPt may be explained qualitatively in terms of the information compiled in Table 3. One expects that slip by unit $1/2 \langle 110 \rangle$ dislocations on either the layered or nonlayered $\{111\}$ planes is the preferred mode. Slip of the type $1/2 \langle 110 \rangle \{111\}$ will be initiated on those planes and in those directions which are most favorably oriented; i.e., those which have the highest Schmidt factor. The necessity of a change in character to superdislocations at order twin boundaries implies that the order twin boundaries are highly effective barriers to slip and must serve as the principle hardening agent at low strains. With continued deformation, slip on the original planes will tend to saturate and may propagate into adjacent order variants in one of three ways: (1) unit slip, (2) superdislocation slip, (3) deformation twinning. All three of these may occur on adjacent $\{111\}$ planes to the initial slip plane. The particular operative mode will depend on the critical stress required to initiate it compared to alternate modes.

The relatively high density of $\{111\}$ deformation twins observed in these samples in comparison to the density of paired dislocations indicates that the required stress to initiate twinning is lower than the critical stress to activate superdislocation sources. This conclusion is very reasonable when one considers that on any given nonlayered

{111} plane, the ratio of superdislocation shears to intrinsic twinning shears is 2:1.

Although it is often assumed that deformation twinning is an unlikely deformation mode in ordered alloys, this particular work as well as that of Pashley *et al.* (10) indicates that it may occur with relative ease in certain neostructural systems. The deformation twins in ordered CuPt were always found to occur by shear on nonlayered planes and were never observed to continue across an order twin boundary uninterrupted. Reference to Figure 1 as well as Table II and Table III shows why this is the case. If the extension of the nonlayered plane of a particular variant is the layered plane in the adjacent variant, deformation is expected to occur only by the more easily activated unit slip. If the extension is a nonlayered plane, the same intrinsic shear would produce the $L1_0$ superlattice structure inside the deformation twins in this new variant. Since this is not energetically feasible, one expects another mode to operate. In general, this new operative mode was found to be slip on an inclined {111} plane.

In summary, it appears that the deformation modes of ordered CuPt in order of preference are (1) $1/2 \langle 110 \rangle$ {111} unit slip on layered or nonlayered planes, (2) {111} deformation twinning on nonlayered planes, (3) slip by $\langle 110 \rangle$ superdislocations on nonlayered planes. The flow stress as a function of order would depend very much on the mechanism of the transformation. For high degrees of order the controlling factor would be the density of order twin boundaries which varies inversely with domain size. For very large domain sizes the ordered alloy may be even softer than the "disordered" alloy quenched from over the

critical temperature (17). In view of the previously discussed results, it is indicative that the critical stresses for slip and twinning shears of a fully ordered alloy are very low in comparison to an alloy containing solid solution effects and short range order.

To make further correlations between deformation mechanisms and strength values it would be necessary to obtain quantitative information regarding critical shear stresses and domain boundary strength. This work is regarded as a first step toward such a correlation by delineating much of the basic deformation processes.

CHAPTER V

RECOMMENDATIONS FOR FUTURE STUDY

This work has illumined the basic deformation mechanisms in ordered CuPt. To achieve a deeper understanding of the mechanical properties of this alloy an understanding of the relationship of the density of order twin boundaries to flow stress and of the exact effect of lattice misfit at the boundaries on dislocation motion would be of value. The effects of misfit on slip and twinning are areas for future research. A knowledge of specific unit and superdislocation interactions on layered and nonlayered slip planes will provide further understanding of slip processes in ordered CuPt.

Deformation twinning is a basic part of the deformation process in ordered CuPt. Little is actually known of the mechanisms of nucleation of deformation twins. With order twin boundaries present in this alloy as convenient nucleation sites, a detailed single crystal study of the deformed alloy may allow knowledge of the nucleation of deformation twinning in face centered cubic alloys.

APPENDIX

IDENTIFICATION OF ORDER VARIANTS IN CuPt FROM
SELECTED AREA DIFFRACTION PATTERNS

Long range ordering occurs in CuPt by the forming of alternate layers of copper and platinum on any of the four $\{111\}$ planes. These variants are identified as Type 1, 2, 3, or 4 according to which $\{111\}$ plane layering occurs on. The specific identities of the four variants are contained in Table I of the Introduction.

Each specific order variant produces its own set of superlattice spots which will appear in certain electron diffraction patterns along with the fundamental lattice spots. A Kikuchi map is shown in Figure 11 with the superimposed low index diffraction patterns which are encountered in this section of the reciprocal space. These patterns contain all the superlattice spots of all four variants.

An examination of these figures reveal that superlattice spots corresponding to specific variants may not be contained in an arbitrarily chosen diffraction pattern. For example, in the (011) pattern only the superlattice spots corresponding to variants type 1 and type 3 can be present, while in the (111) and (001) patterns no superlattice spots appear at all. Therefore the unambiguous identification of an order variant can be extracted from a selected area diffraction pattern only if superlattice spots appear. Further inspection shows that only the (111) and (001) patterns contain no superlattice spots, and that in all other patterns shown, only two of the four variants superlattice spots

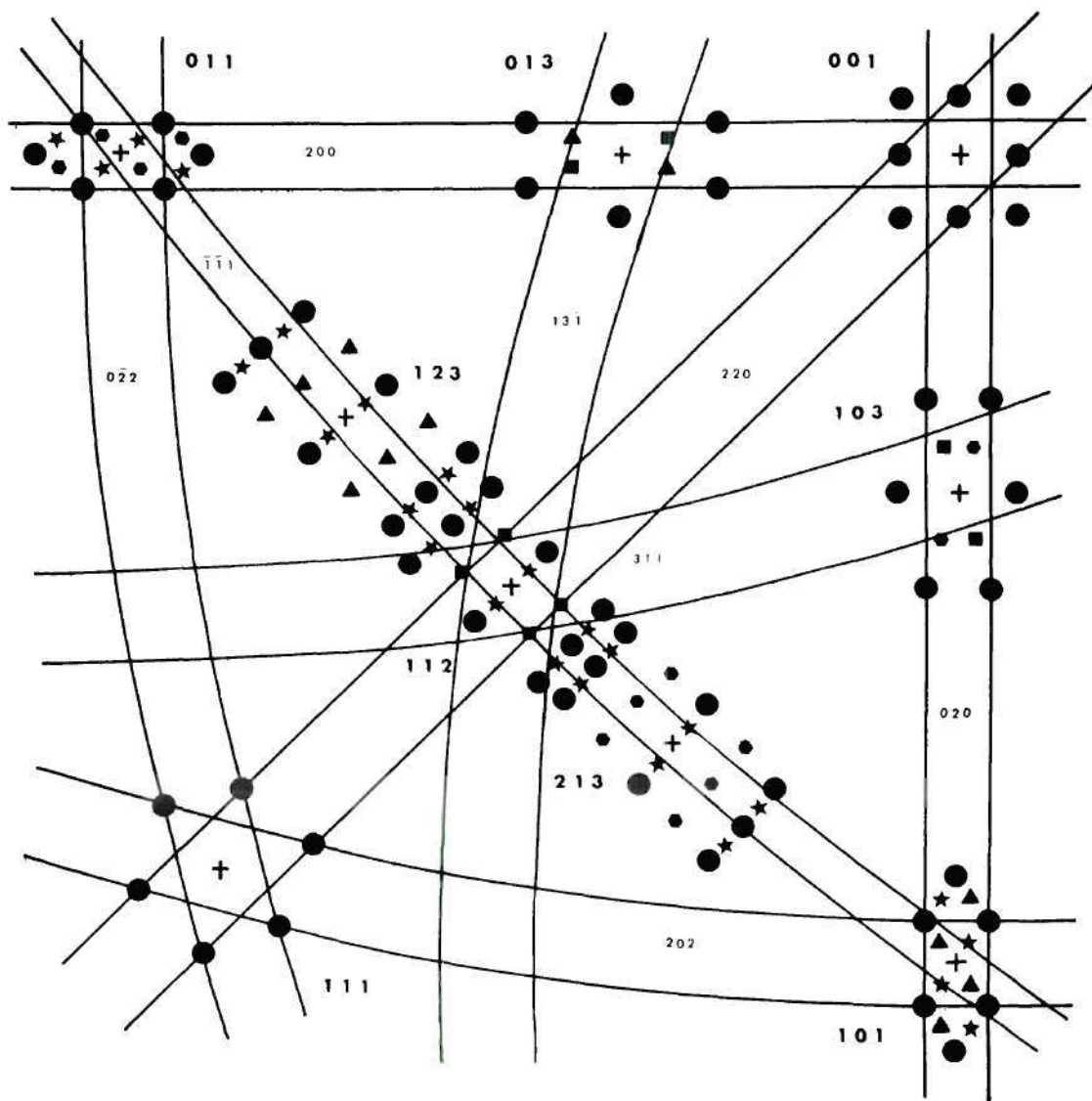
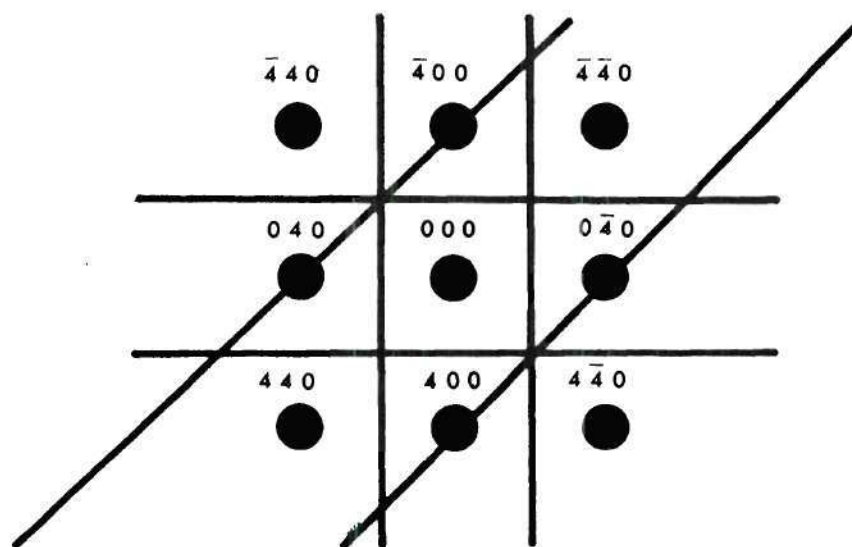


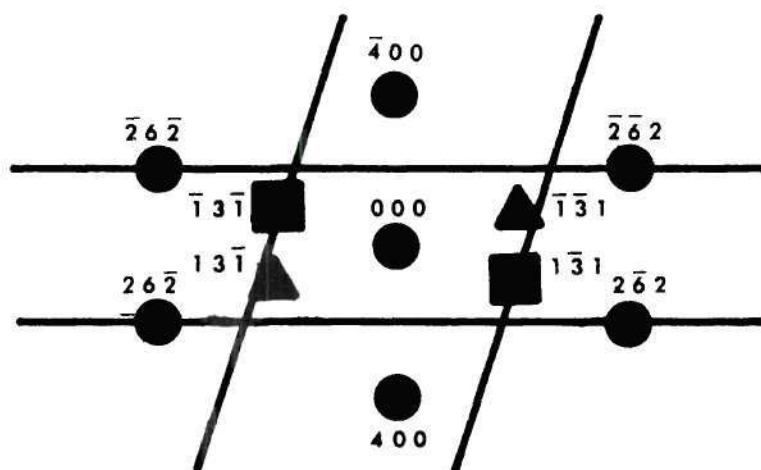
Figure 11. A Kikuchi Map of the Ordered CuPt Reciprocal Space, Viewing the Ewald Sphere from Inside.

(a) The Positive Octant.

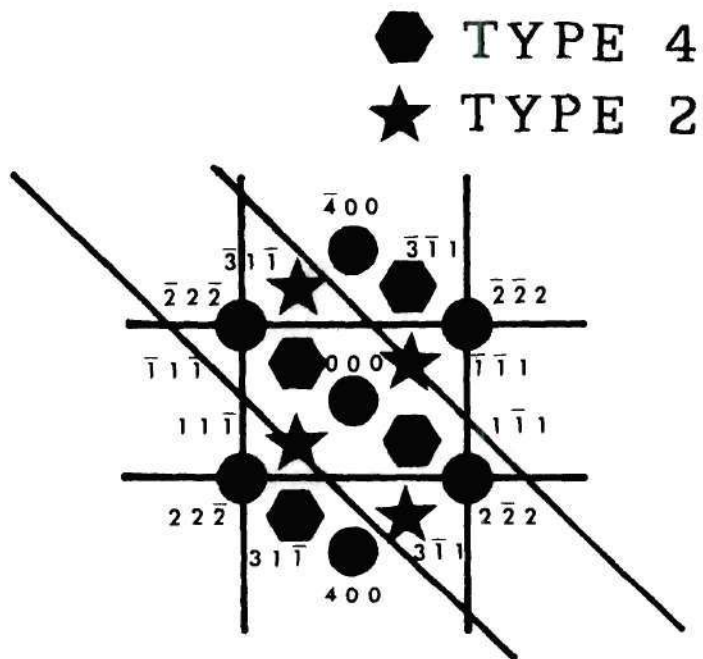


a) 001

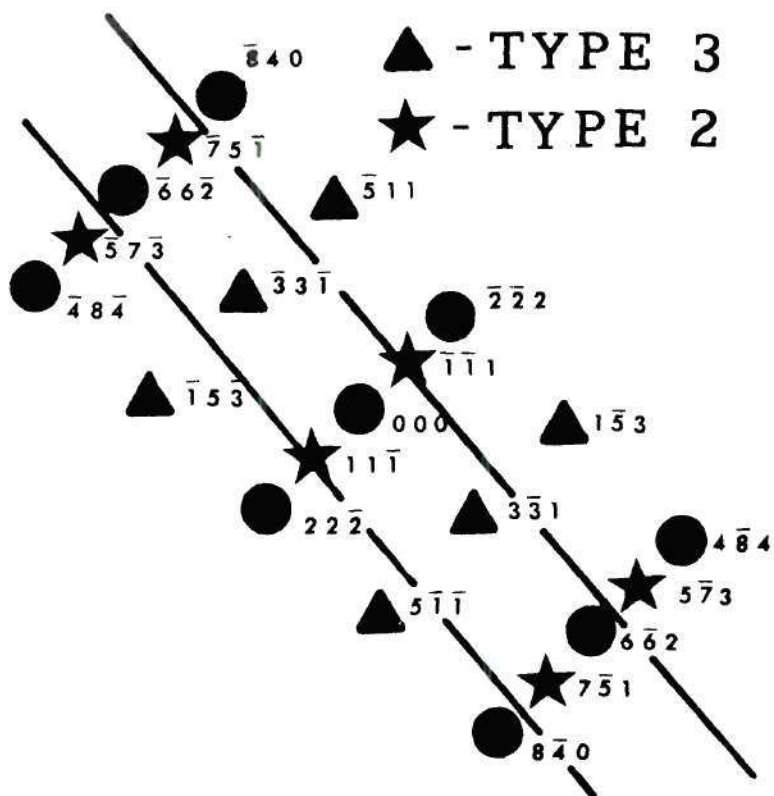
■ TYPE 1
▲ TYPE 3



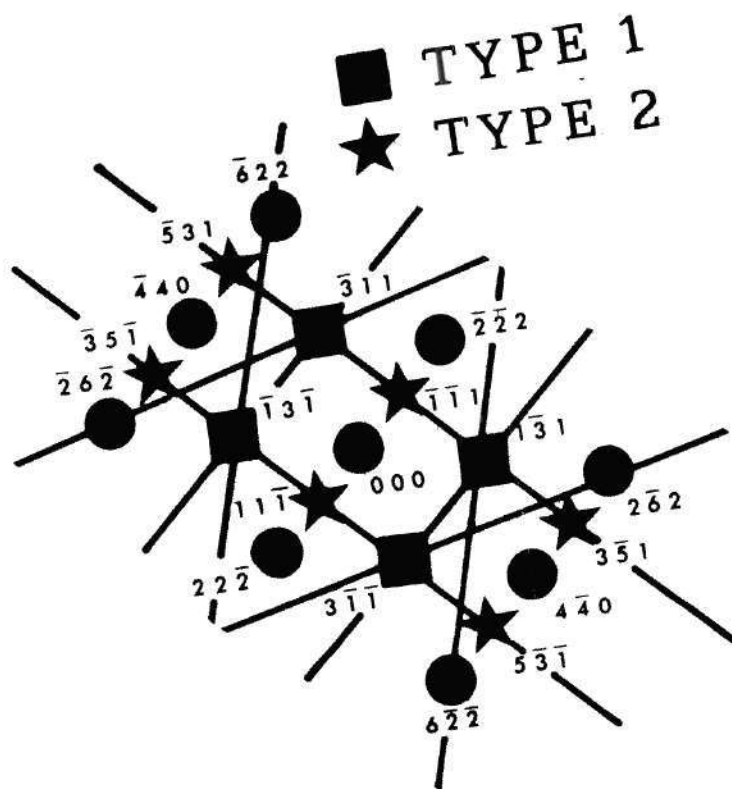
b) 013



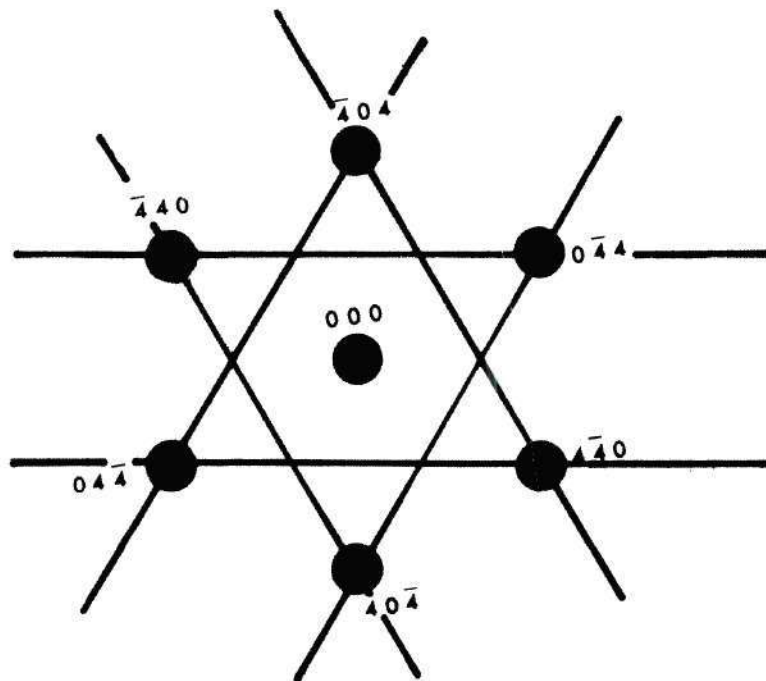
c) 011



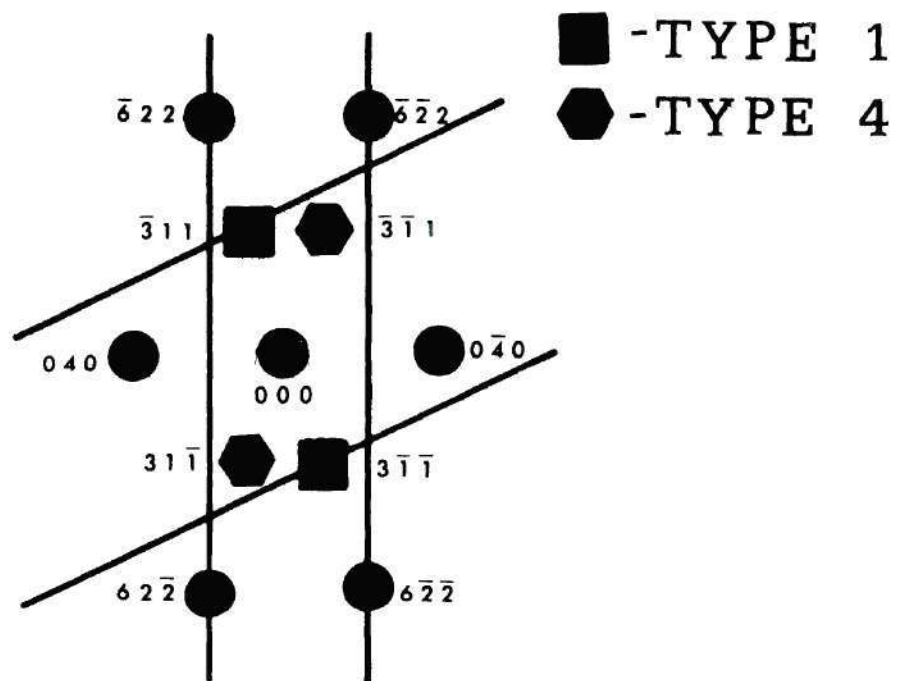
d) 123



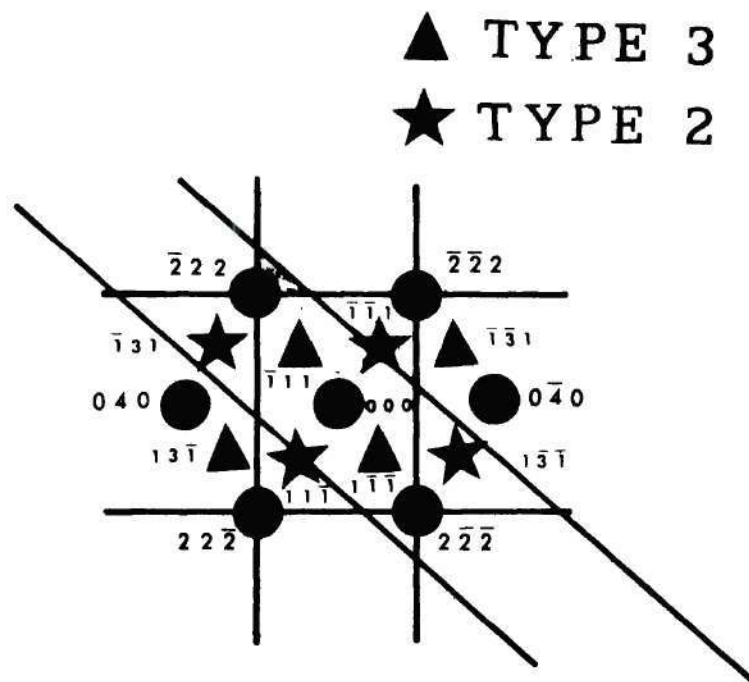
e) $11\bar{2}$



f) $11\bar{1}$

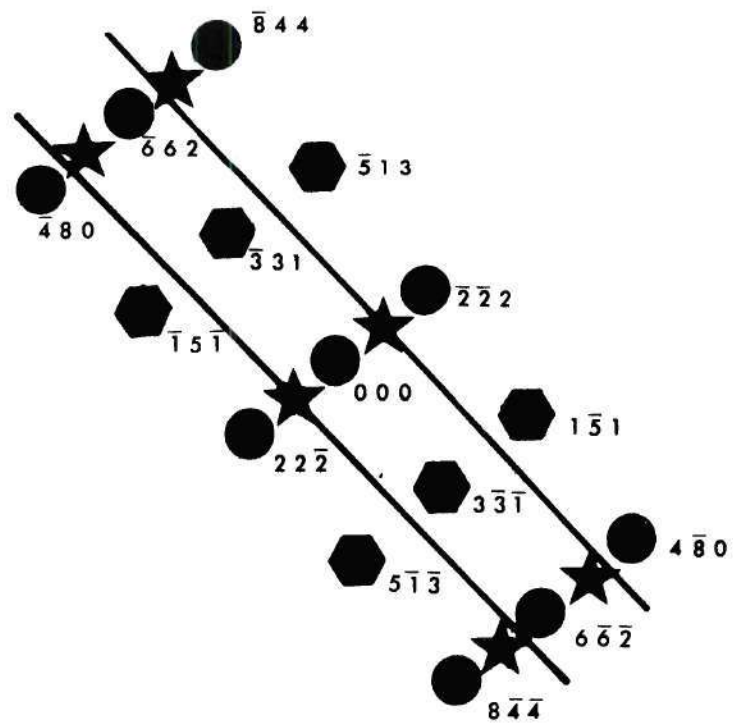


g) 103



h) 101

★ TYPE 2
 ● TYPE 4



i) **213**

may appear in any one of the patterns. It is necessary to view only two of these patterns to uniquely identify an order variant from which the patterns were taken. The manner in which this is done is shown by the logic diagrams of Figures 12 and 13. The starting orientations are (011) and (112) respectively, which are the most commonly observed patterns in this material.

To make an identification by the above technique it is necessary to tilt through several degrees along one of the Kikuchi bands shown in Figure 11. A number of difficulties associated with both samples preparation and the construction of the Swann stage make smooth tilting from one orientation to another difficult. (Unique identification by the above method could not be achieved in every case.)

The analyses used in this study were concerned with the identification of order twins adjacent to an order twin boundary. If either one of the variants can be identified, the identity of the second variant often can be inferred from the orientation of the order twin boundary. This is feasible because the coherent boundary between any two variants is restricted to one of two possibilities as shown in Table 4. If the boundary follows the anticipated orientation and if the trace analysis is not ambiguous, this technique can be used to obtain additional information.

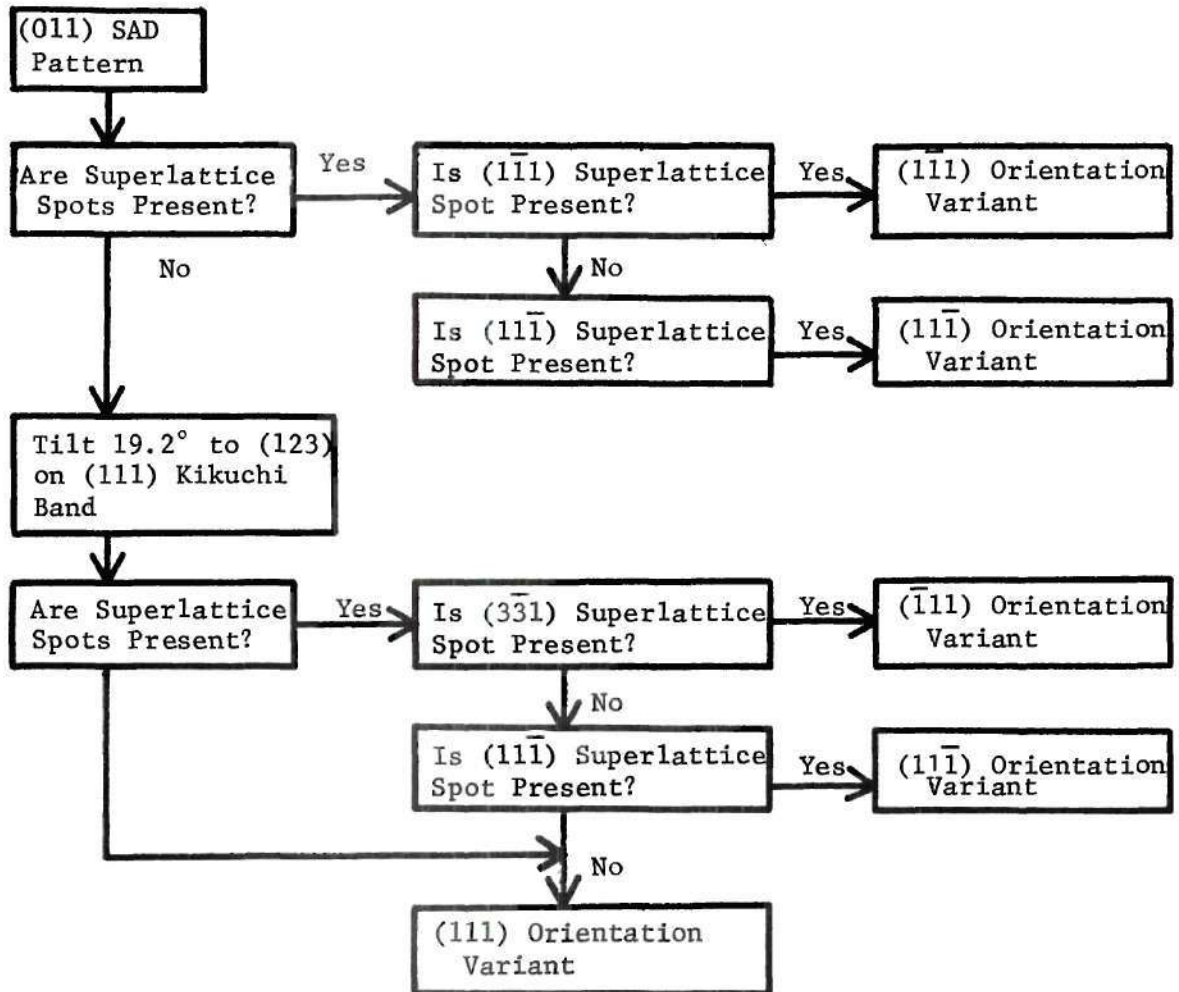


Figure 12. Identification of Orientation Variants in Ordered CuPt Using (011) and (123) Selected Area Diffraction Patterns.

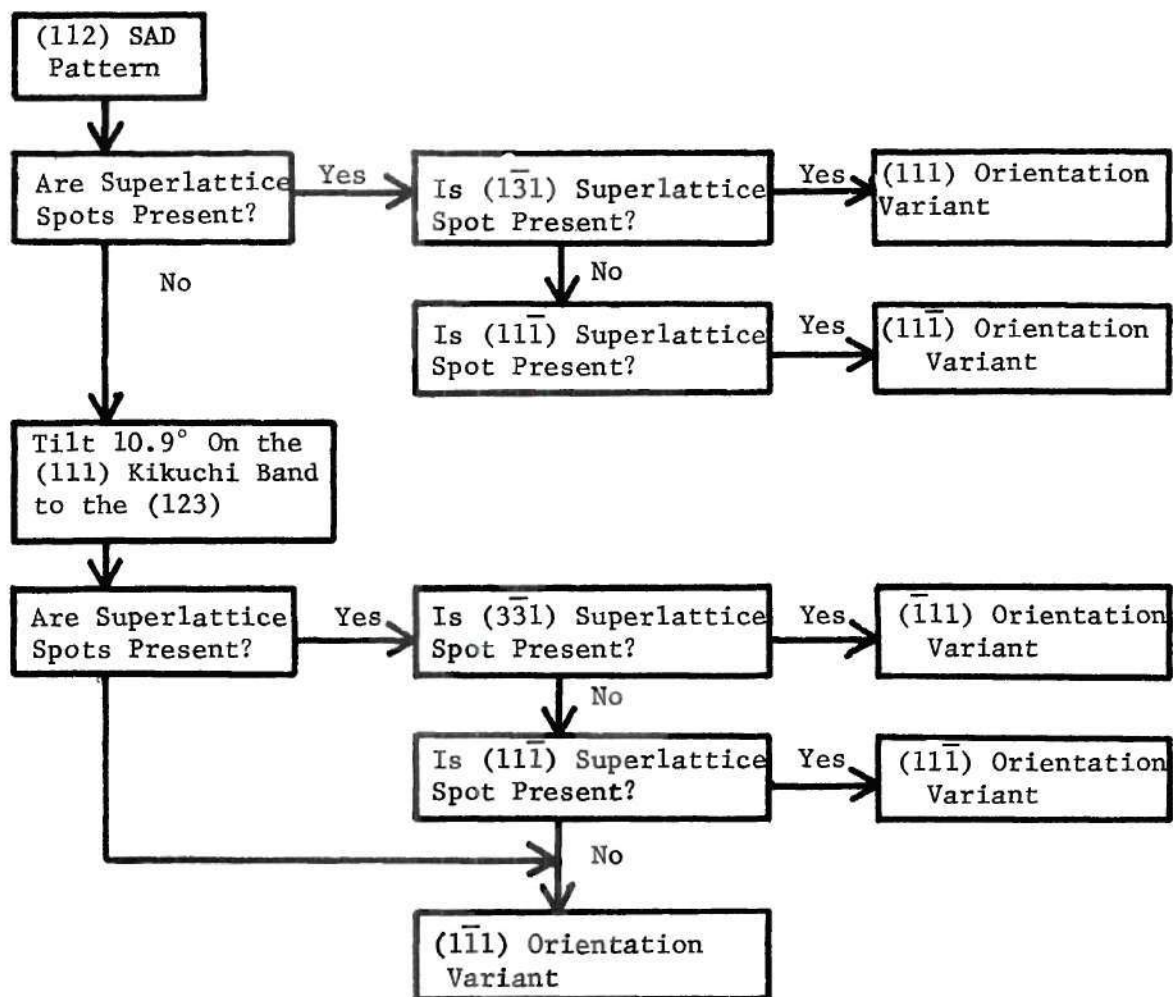


Figure 13. Identification of Orientation Variants in Ordered CuPt Using (112) and (123) Selected Area Diffraction Patterns.

Table 4. Orientation of Coherent Interfaces Between Adjacent Order Variants.

Advacent Variants	Orientation of OTB
Type 1 and Type 2	(110) or (001)
Type 1 and Type 3	(011) or (100)
Type 1 and Type 4	(101) or (010)
Type 2 and Type 3	($\bar{1}01$) or (010)
Type 2 and Type 4	(01 $\bar{1}$) or (100)
Type 3 and Type 4	($\bar{1}10$) or (001)

BIBLIOGRAPHY

1. C. Barrett and T. B. Massalski, Structure of Metals (McGraw-Hill, Inc., New York, 1966).
2. L. Guttman, "Order-Disorder Phenomena in Metals", Solid State Physics 3 (Academic Press, New York, 1956) 145.
3. N. S. Stoloff and R. G. Davies, "The Mechanical Properties of Ordered Alloys", Progress in Materials Science 13, No. 1 (Pergamon Press, Oxford, 1966) 3.
4. W. L. Bragg and E. J. Williams, Proc. Roy Soc., A145, (1934) 699 and A151, (1935) 540.
5. A. G. Guy, Elements of Physical Metallurgy (Addison-Wesley, Reading Massachusetts, 1967) 460.
6. J. S. Bowles and A. S. Malin, Journal of the Australian Institute of Physics 5 (1966) 131.
7. L. E. Tanner, Physica Status Solidi 30 (1968) 685.
8. L. E. Tanner, "The Ordering of Ni₂V -- Initial Observations", Ordered Alloys -- Structural Applications and Physical Metallurgy, presented at the Third Annual Bolton Landing Conference, Lake George, New York, Sept. 8-10, 1969 (Claitor's Publishing Division, Baton Rouge, La., 1970) 253.
9. Richard Mitchell, Master's Thesis, Georgia Institute of Technology, 1972.
10. D. W. Pashley, J. L. Robertson, and M. J. Stowell, Phil. Mag. 19 (1969) 83.
11. H. G. Paris, and B. G. LeFevre, Mat. Res. Bul. 7 (1972) 1109.
12. R. W. Cahn, "Correlation of Local Order with Mechanical Properties", Local Atomic Arrangements Studied by X-ray Diffraction, edited by J. B. Cohen and J. E. Hillard (Gordon and Breach, New York, 1966) 179.
13. J. B. Cohen, J. Mat. Sci. 4 (1969) 1012.
14. C. H. Johansson and J. O. Linde, Annalen der Physik, 82 (1927) 459.
15. C. B. Walker, J.A.P. 23 No. 1 (1952) 118.

16. R. W. Cahn, private communication, to be published in Acta. Met.
17. R. Mitchell, H. G. Paris, and B. G. LeFevre, Met. Trans. 4 (1973) 833.
18. N. T. Corke, S. Amelinckx, and J. Van Landuyt, Mat. Res. Bul. 4 (1969) 289.
19. M.A.P. Dewey and J. G. Lewis, J. Sci. Inst. 40 (1963) 385.
20. C.K.H. Dubose and J.O. Steigler "Semi Automatic Preparation of Specimens for T.E.M." ORNL 4066 (Feb. 1967).
21. P. B. Hirsch, A. Howie, R. B. Nicholson, D. W. Pashley, M. J. Whelan, Electron Microscopy of Thin Crystals (Butterworths, London, 1965).
22. L. E. Murr, Electron Optical Applications in Materials Science, (McGraw-Hill Book Co., New York, 1970).
23. G. Thomas, Transmission Electron Microscopy of Metals (John Wiley and Sons, New York, 1962).
24. A. Howie, PhD Thesis, University of Cambridge, 1960.
25. J. A. Venables, Phil. Mag. 6 (1961) 379.